

Particle transport in low-energy ventilation systems. Part 2: Transients and experiments

Abstract Providing adequate indoor air quality while reducing energy consumption is a must for efficient ventilation system design. In this work, we study the transport of particulate contaminants in a displacement-ventilated space, using the idealized ‘emptying filling box’ model (P.F. Linden, G.F. Lane-serff and D.A. Smeed (1990) Emptying filling boxes: the fluid mechanics of natural ventilation, *J. fluid Mech.*, **212**, 309–335.). In this paper, we focused on transient contaminant transport by modeling three transient contamination scenarios, namely the so called ‘step-up’, ‘step-down’, and point source cases. Using analytical integral models and numerical models we studied the transient behavior of each of these three cases. We found that, on average, traditional and low-energy systems can be similar in overall pollutant removal efficiency, although quite different vertical gradients can exist. This plays an important role in estimating occupant exposure to contaminant. A series of laboratory experiments were conducted to validate the developed models.

D. T. Bolster, P. F. Linden

Department of Mechanical and Aerospace Engineering,
University of California, San Diego, La Jolla, CA, USA

Key words: Low-energy ventilation; Contaminant; Particles.

Diogo T. Bolster
Department of Geo-Engineering
Technical University of Catalunya (UPC)
Campus Road
08034 Barcelona
Spain
Tel.: +34 655 039 065
Fax: +34 944 016 890
e-mail: diogobolster@gmail.com, dbolster@ucsd.edu

Received for review 21 January 2008. Accepted for
publication 4 August 2008.
© Indoor Air (2008)

Practical Implications

The results presented here illustrate that the source location plays a very important role in the distribution of contaminant concentration for spaces ventilated by low energy displacement-ventilation systems. With these results and the knowledge of typical contaminant sources for a given type of space practitioners can design or select more effective systems for the purpose at hand.

Introduction

Buildings and occupied spaces are transient by their nature as people move, equipment is turned on and off, external conditions change, etc. While making a steady-state assumption is often useful in the initial study of contaminant distribution (Musser and Persily, 2002) it does not provide all the information as it neglects the temporal nature of contaminant sources and building ventilation rates (e.g. Bolster and Caulfield, 2008).

In general, an efficient manner of air quality control is to remove the contaminant before it has time to mix throughout the space, which means extracting it from near the source, where the concentration will be the highest. Therefore, it is

important to understand how the contaminant will disperse in the room. In most indoor environments the transport of the pollutant is advective, as the diffusion rate is relatively small. An approximate diffusion timescale is 5 days for a typical space, yet from experience we know that the actual dispersion rate is more on the order of minutes or hours depending on the space in question. As such understanding the temporal nature of this dispersion can provide some useful insight into effective removal of indoor air contaminants.

Much previous work has been carried out in the field of contaminant modeling in buildings. Most of it is based on reduced order zonal models (Feustel, 1999; Schneider et al., 1999; Zhao et al., 2004). In zonal models, buildings are typically broken into several

zones, which interact with one another. Each of the zones is assumed to be well mixed at all times.

This approximation of uniform and instantaneous mixing is very convenient and can often be justified for cases with strong internal air motion. However, this assumption may not always be appropriate, particularly in low-energy ventilation systems where there is a deliberate creation of non-uniformity in temperature. In such cases, exposure to the contaminants may depend significantly on a person’s location with a space. Ozkaynak et al. (1982) found that pollutant levels in a kitchen with the oven on depended heavily on the sampling location. Rodes et al. (1991) discovered that personal sampling almost always reveals a higher exposure to contaminants that would be predicted from indoor air monitoring that assumes perfect mixing. Lambert et al. (1993) showed that the levels of suspended particles in a non-smoking section of a restaurant were 40–65% less than that in the smoking section.

Various computational fluid dynamics (CFD) studies have been conducted looking at particulate transport in ventilated spaces (e.g. Holmberg and Li, 1998; Zhang and Chen, 2006; Zhao et al., 2004). However, even with current computer speeds, full-scale simulations can be prohibitively expensive, particularly for large buildings with multiply connected spaces. Accurate CFD simulations of such flows can be very difficult, because of uncertain boundary conditions (Cook et al., 2003), the difficulties involved in accurately modeling thermal plumes (Yan, 2007) and the appropriate selection of a wide choice of available turbulence models (Ji et al., 2007), which can all affect the flows involved in a non-negligible manner.

Reduced analytical models (such as the one we present in this paper) can be useful, as they can be integrated into zonal computer models (e.g. Energy-Plus; Department of Energy, Berkeley, CA, USA) where connected spaces are treated as nodes that communicate with one another via conservation equations (e.g. temperature, contaminant concentration, etc.). Further, such analytical models provide important benchmarks, necessary for the validation of CFD models. Also, while useful for specific cases, CFD studies do not always provide practical information about the general physics and behavior of contaminants in low-energy ventilation systems.

In this work, we compare contaminant transport in a traditional ‘mixing’ system model with two low-energy ‘displacement’ ventilation models using reduced analytical integral models to study the average concentrations as they vary with time. We then use a numerical model (Germeles, 1975) to study the detailed vertical distribution of contaminant. These models are then compared with the results of laboratory experiments to validate the information obtained with the mathematical models.

Mathematical models

To understand the fate of particles in a ventilated space it is necessary to understand the flow within the space. We consider three models, which are shown schematically in Figure 1. We analyze two low-energy ventilation models [(b) and (c)] and one traditional mixing model (a). In the low-energy models we consider the space either mechanically or naturally ventilated with fresh air entering through a low-level vent and hot buoyant air leaving via a vent at high level. Heat sources in the space are represented by ideal plumes.

Contamination scenarios considered

For each of the models depicted in Figure 1, we consider three types of contamination situations:

1. Step-down (natural attenuation): This is the situation where a space is initially uniformly filled with a contaminant and fresh, uncontaminated air is introduced into the space.
2. Step-up (external contaminant): Here we consider a space that is initially uncontaminated. Then a contaminant is introduced in through the ventilation system. At steady state this scenario is equivalent to the external contaminant source considered in Part 1 of this work.
3. Isolated source in plume: Here we consider a space that is initially uncontaminated. Then a contaminant is introduced as a point source located within the plume. We choose this location because people are often the source of heat as well as the source of contaminants in buildings. In addition, it is also the only type of point source that we can currently adequately describe with our model. At steady state, this scenario is equivalent to the internal contaminant source considered in Part 1 of this work.

Model (a) – entirely well-mixed space

In this model, we treat the entire room as well mixed (Figure 1a). The concentration in a well-mixed space, K_{wm} , satisfies the conservation equation

$$\frac{dK_{wm}}{dt} = -\frac{Q_{in} + Q_{fall}}{SH} K_{wm} + \frac{Q_{in}}{SH} K_{in} + \frac{Q_{in}K_s}{SH}, \quad (1)$$

where Q_{in} is the flow rate into the space, $Q_{fall} = v_{fall} S$ is defined as the settling flow rate, v_{fall} is the settling velocity, assumed here to be the Stokes settling velocity, K_{in} is the concentration of contaminant in the incoming air, K_s is the concentration associated with a point source, S is the room cross sectional area, and H is the height of the room. Q_{fall} quantifies the amount of deposition that will take place. We neglect deposition of particles to the ceiling and sidewalls and assume that particles settle out of the lower and upper

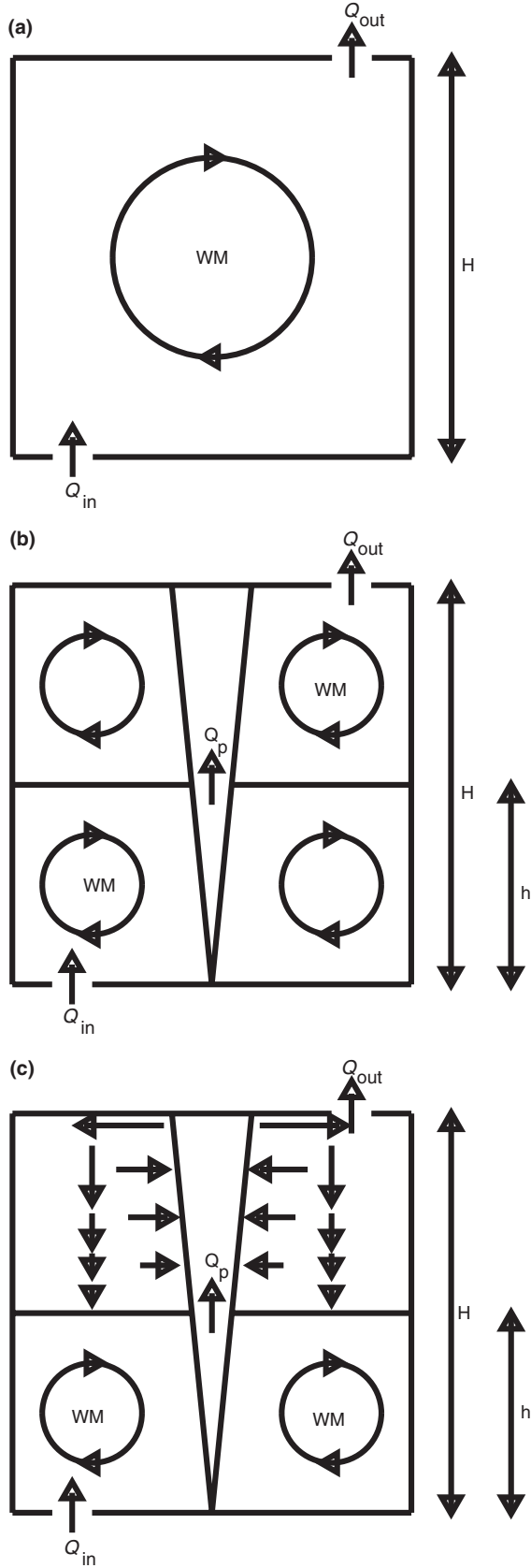


Fig. 1 Models of displacement ventilation systems. (a) Single well-mixed layer, (b) two well-mixed layers, and (c) two-layer model with well-mixed lower layer and unmixed upper layer. WM stands for well mixed

layers at this settling velocity. While this is a strong assumption, in Part 1 of this work we illustrated that this assumption, while providing quantitatively different results, still allows for detailed qualitative analysis.

Model (b) – well-mixed two-layer model

In this section, we consider model (b) from Figure 1. We take an approach similar to that of Hunt and Kaye (2006) and assume that the upper and lower layers are always well mixed. Thus, the governing equations for conservation of contaminant in each of the layers are

$$\frac{dK_l}{dt} = -\left(\frac{Q_p + Q_{fall}}{Sh}\right)K_l + \frac{Q_{fall}}{Sh}K_u + \frac{Q_{in}}{Sh}K_{in}$$

$$\frac{dK_u}{dt} = \frac{Q_p}{S(H-h)}K_l - \left(\frac{Q_{fall} + Q_p}{S(H-h)}\right)K_u + \frac{Q_p K_s}{S(H-h)} \quad (2)$$

where K_l and K_u are the concentrations of contaminant in the lower and upper layers respectively, h is the height of the lower layer, and Q_p is the plume flow rate across the interface and at steady state $Q_p = Q_{in}$.

Model (c) – mixed lower layer, unmixed upper layer

Here we consider model (c) from Figure 1. For a well-mixed lower layer and unmixed upper layer the conservation equations for the upper and lower layer are slightly modified from the previous section. Instead of removing fluid of the average concentration of contaminant, we must now account for the fact that the upper layer can have concentration gradients in it, thus leading to the following conservation equations

$$\frac{dK_l}{dt} = -\left(\frac{Q_p + Q_{fall}}{Sh}\right)K_l + \frac{Q_{fall}}{Sh}K_u(z=h) + \frac{Q_{in}}{Sh}K_{in},$$

$$\begin{aligned} \frac{d\bar{K}_u}{dt} = & \frac{Q_p}{S(H-h)}(K_l - K_u(z=H)) \\ & - \left(\frac{Q_{fall}}{S(H-h)}\right)K_u(z=h) + \frac{Q_p K_s}{S(H-h)}. \end{aligned} \quad (3)$$

To understand the dynamics of the upper layer it is important to understand the flow within the space, which is determined by coupling the plume flow with the environment outside the plume. Exact details of this are given in Bolster and Linden (2007).

Non-dimensionalization

We non-dimensionalize as follows:

$$t = \tau \frac{SH}{Q_p}, \quad K = K_{ref}\kappa, \quad h = H\zeta, \quad (4)$$

where K_{ref} is a reference concentration, which will be different for each of the three situations considered. Here τ , κ , and ζ are dimensionless time, dimensionless concentration, and dimensionless interface height, respectively. For the step-down method, it is the initial concentration of contaminant in the space ($K_{\text{ref}} = K_0$). For the step-up system, it is the concentration of contaminant entering the spaces ($K_{\text{ref}} = K_{\text{in}}$) and for the point source case, it is the concentration of the source ($K_{\text{ref}} = K_s$). This results in the following dimensionless equations:

$$(a) \quad \frac{d\kappa}{d\tau} = -(1 + \alpha)\kappa + \kappa_{\text{in}} + \kappa_s, \quad (5)$$

$$(b) \quad \frac{d\kappa_l}{d\tau} = \frac{-(1 + \alpha)\kappa_l + \alpha\kappa_u + \kappa_{\text{in}}}{\zeta},$$

$$\frac{d\kappa_u}{d\tau} = \frac{\kappa_l - (1 + \alpha)\kappa_u + \kappa_s}{1 - \zeta}, \quad (6)$$

Results

All of the above equations are linear and can be solved analytically. In this section, we present the general solutions to the governing equations without considering the specific contamination conditions. The contamination scenarios mentioned previously will be discussed later in this section.

General results of model equations

Model (a). The governing equation (5), can be integrated to give the average concentration throughout the room. It is described by a simple exponential equation

$$\kappa^{(a)} = \kappa_o e^{-(1+\alpha)\tau} + \frac{\kappa_{\text{in}} + \kappa_s}{1 + \alpha} (1 - e^{-(1+\alpha)\tau}), \quad (8)$$

where κ_o is the initial contaminant concentration in the room, and κ_{in} is the concentration of contaminant entering the room.

Model (b). The system of equations (6), can be solved by Laplace transforms or as an eigenvalue problem. The solution is

$$\kappa_l^{(b)} = \frac{(1 + \alpha)\kappa_{\text{in}} + \alpha\kappa_s}{\alpha^2 + \alpha + 1} + e^{-\frac{(1+\alpha)}{2\zeta(1-\zeta)}\tau} \left(\left(\kappa_o - \frac{(1 + \alpha)\kappa_{\text{in}} + \alpha\kappa_s}{\alpha^2 + \alpha + 1} \right) \cosh\left(\frac{A_1 \tau}{2\zeta(1 - \zeta)}\right) + \frac{\kappa_o(\alpha - 1 + 2\zeta)(\alpha^2 + \alpha + 1) + \kappa_{\text{in}}(\alpha^2 + 1 - 2\zeta(\alpha^2 + \alpha + 1)) - \kappa_s(\alpha^2 + \alpha)}{A(\alpha^2 + \alpha + 1)} \sinh\left(\frac{A_1 \tau}{2\zeta(1 - \zeta)}\right) \right), \quad (9)$$

$$\kappa_u^{(b)} = \frac{\kappa_{\text{in}} + (1 + \alpha)\kappa_s}{\alpha^2 + \alpha + 1} + e^{-\frac{(1+\alpha)}{2\zeta(1-\zeta)}\tau} \left(\left(\kappa_o - \frac{\kappa_{\text{in}} + (1 + \alpha)\kappa_s}{\alpha^2 + \alpha + 1} \right) \cosh\left(\frac{A_1 \tau}{2\zeta(1 - \zeta)}\right) + \frac{\kappa_o(\alpha + 1 - 2\zeta\alpha)(\alpha^2 + \alpha + 1) + \kappa_{\text{in}}(-1 - \alpha) - \kappa_s(\alpha^2 + 2\alpha + 1 - 2\zeta(\alpha^2 + \alpha + 1))}{A(\alpha^2 + \alpha + 1)} \sinh\left(\frac{A_1 \tau}{2\zeta(1 - \zeta)}\right) \right), \quad (10)$$

$$(c) \quad \frac{d\bar{\kappa}_l}{d\tau} = \frac{\alpha}{\zeta} (\kappa_u(\zeta = \zeta_h) - \bar{\kappa}_l) + \frac{1}{\zeta} (\kappa_{\text{in}} - \bar{\kappa}_l),$$

$$\frac{d\bar{\kappa}_u}{d\tau} = \frac{-\alpha}{1 - \zeta} (\kappa_u(\zeta = \zeta_h)) + \frac{1}{1 - \zeta} (\bar{\kappa}_l - \kappa_u(\zeta = 1) + \kappa_s). \quad (7)$$

where $\alpha = Q_{\text{fall}}/Q_p$, which is a dimensionless representation of the particle settling velocity.

where

$$A_1 = \sqrt{1 + 2\alpha + \alpha^2 + 4\zeta^2 + 4\zeta^2\alpha + 4\zeta^2\alpha^2 - 4\alpha\zeta - 4\zeta - 4\zeta\alpha^2}. \quad (11)$$

Model (c). To close this system of equations (7), we must find analytical expressions for $\kappa_u^{(c)}(\zeta = \zeta_h, t)$ and $\kappa_u^{(c)}(\zeta = 1, t)$. It is necessary to examine the full temporal evolution of the contaminant transport to determine these quantities.

In the limit of $\alpha \rightarrow 0$, $\kappa_{in} = 0$, and in the current non-dimensionalization this solution collapses to that of Hunt and Kaye (2006). Also, at steady state, all the results presented in Part 1 of this work are recovered.

Because diffusion is being neglected due to high Peclet numbers, the method of characteristics can be used to determine the concentration of contaminant in the upper layer at the interface height. This concentration will be that at the top of the room a period τ_d earlier, where τ_d is the time taken for a front of descending particles to travel from the top of the room to the interface. It can be shown that

$$\tau_d = \frac{3}{5} \zeta_h \ln \left(\frac{1 - (1 - \frac{3}{5}\alpha)\zeta_h}{\zeta - (1 - \frac{3}{5}\alpha)\zeta_h} \right). \quad (12)$$

Therefore, to close this system of equations, the only quantity required is an estimate of the contaminant concentration at the top of the room. Assuming that the plume spreads instantaneously across the entire plan area of the ceiling, and that a perfectly mixed layer forms, we can equate the background concentration to that of the plume at the top of the room (see Appendix A).

$$\kappa_u^{(c)}(\zeta=1, \tau) = \frac{5(1-\zeta_h)\bar{\kappa}_u(\tau) + 3(\bar{\kappa}_1(\tau) + \kappa_s)\zeta_h}{5-2\zeta_h} \left(\frac{1}{1 + \frac{3\alpha\zeta}{5-2\zeta}} \right)$$

$$\kappa_u^{(c)}(\zeta_h, \tau) = \kappa_u^{(c)}(\zeta = 1, \tau - \tau_d). \quad (13)$$

An analytical solution to this system of equations has been found and can be computed. However, it is very laborious and involves many summations which must be computed and gives very little insight into the physical behavior of the system. Instead, the equations are solved numerically using a Runge–Kutta scheme, which is more efficient. The solutions of the numerical and analytical systems are identical.

Step-down

Here we consider the removal of a uniformly distributed contaminant from the space by introducing uncontaminated air in through the ventilation system. In this case, $\kappa_{in} = 0$, $\kappa_o = 1$, and $\kappa_s = 0$ which can be substituted into the results presented in the previous section ‘General results of model equations’. Figure 2 displays a sample of solutions for the average

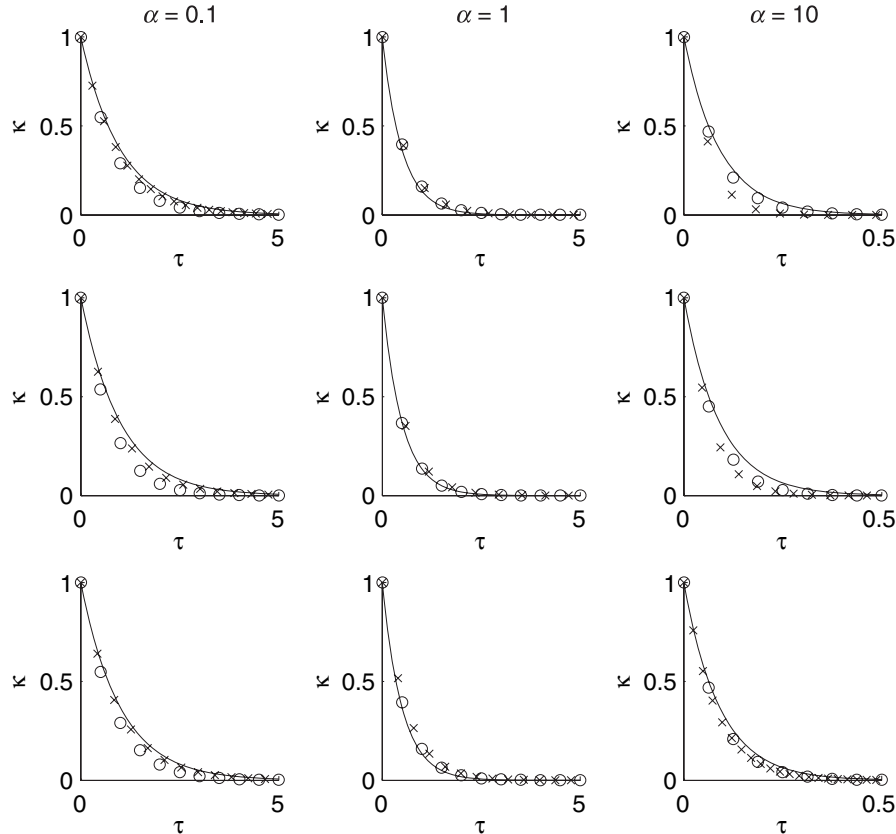


Fig. 2 Step-down case – average concentration for three model with various α and ζ . One-layer well mixed (–), two-layer well mixed (o), two-layer unmixed (x). The top row corresponds to $\zeta = 0.25$, the middle row to $\zeta = 0.5$, and the bottom row to $\zeta = 0.75$

contaminant concentration for each of the three models at three values of interface height, $\zeta = 0.25, 0.5$ and 0.75 , and three values of $\alpha = 0.1, 1$ and 10 . Except for the case of $\alpha = 10$ and $\zeta = 0.25$ the average amounts of contaminant are similar for the three cases, suggesting that each system exhibits comparable efficiency vis-a-vis overall contaminant removal. This conclusion applies over a wide range of parameter space corresponding to typical physical situations. Although the average concentrations are approximately the same, this does not imply that the vertical concentration profiles are also the same, merely that the concentration being extracted is similar. In the next section of the paper, we study these vertical concentration profiles.

Quantity of particulates deposited. A quantity that may be useful to know is the percentage of particulate contaminants that escape the room through the upper vent and the percentage that is deposited on the floor. The percentage of contaminant deposited, Γ_{dep} , can be found as the integral of the product concentration and settling flow rate over time

$$\Gamma_{\text{dep}} = \int_0^{\tau \rightarrow \infty} \kappa_1(\tau') \alpha \zeta d\tau'. \quad (14)$$

The quantity Γ_{dep} is a measure of the percentage of contaminant that a person occupying the lower layer will be exposed to, as all deposition occurs in the lower layer.

Figure 3 displays Γ_{dep} for all three models over a wide range of parameter space. The quantitative values of Γ_{dep} are roughly similar for the three cases; although, there are interesting qualitative differences. For the two-layer models, (b) and (c), there is a monotonic increase in Γ_{dep} as ζ increases. For the unmixed upper layer, the quantity of deposited contaminant is always smaller than for the well-mixed two-layer system. As shown in Bolster and Linden (2007), where we compare the effective draining rates of the upper and lower layers of both these systems, it can be shown that the unmixed upper layer case is less effective at removing contaminant from the upper layer. The mechanism of contaminant removal is the same here and, in addition, there is transport back down to the lower layer from the upper layer because of settling. This leads to the larger quantities of deposition observed in model (c). The largest differences in Γ_{dep} between models (b) and (c), equal to 0.11, occurs for $\zeta = 0.35$ and $\alpha = 2$. A contour plot of these differences is shown in Figure 4.

Figure 5 compares Γ_{dep} for the single-layer well-mixed space to the two-layer models. The line where the predicted amount of deposition is equal for both models is shown on each plot. For smaller particles (i.e. α small) and lower interfaces (i.e. ζ small), the two-

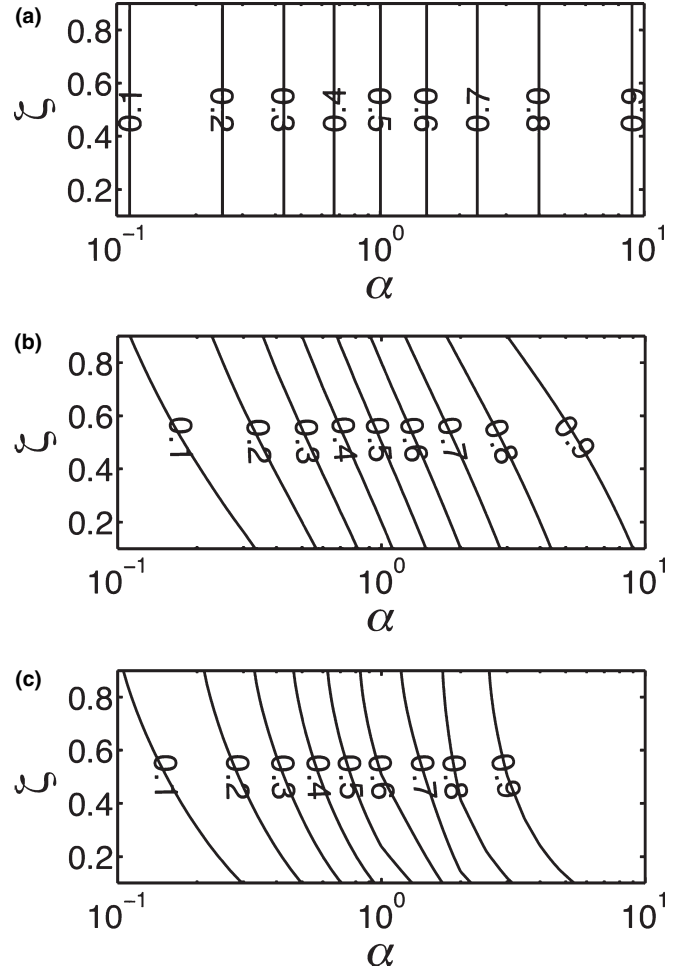


Fig. 3 Isocontours of the fraction of total initial particles that are deposited on the floor during a step-down study for various values of α and ζ for each of the three models, (a–c), considered here

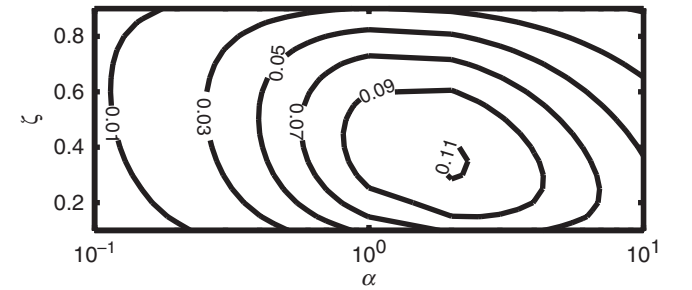


Fig. 4 Isocontours for a range of α and ζ of the difference in the fraction of deposited particles during a step-down study between models (c) and (b) $\Gamma_{\text{dep}}^c - \Gamma_{\text{dep}}^b$

layer systems predict lower values of Γ_{dep} , while for larger values of these parameters the single well-mixed space predicts lower values. As Γ_{dep} is effectively a measure of the quantity of contaminant that occupants in the lower layer have been exposed to, this plot shows that for certain locations of interface and particle sizes, the low-energy systems reduce exposure. However, for

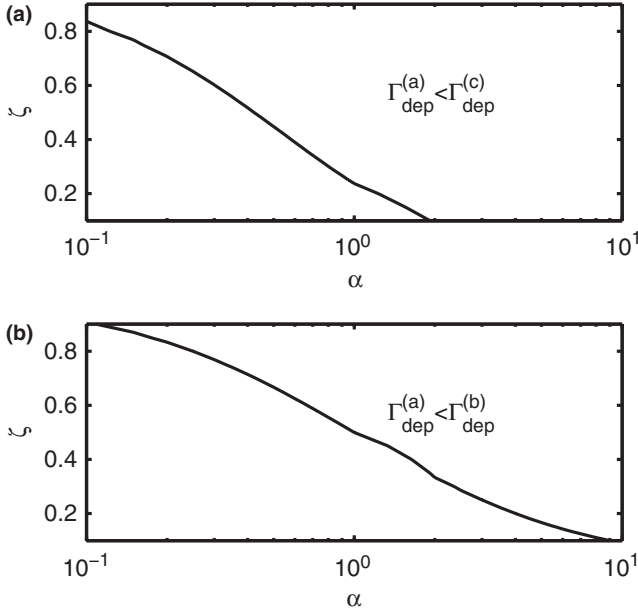


Fig. 5 Comparison of Γ_{dep} for the single-layer well-mixed space to the two-layer models. (a) To the right of the line $\Gamma_{\text{dep}}^a < \Gamma_{\text{dep}}^c$ (b) To the right of the line $\Gamma_{\text{dep}}^a < \Gamma_{\text{dep}}^b$

larger particles and higher interfaces, the traditional mixing ventilation system outperforms the low-energy systems.

Step-up

Now we consider the opposite situation, where a room is initially completely uncontaminated and a contaminant is introduced via the ventilation system. This can correspond to a number of scenarios, such as a leak in a ventilation system, a malicious release, or an external contaminant entering the building through natural ventilation.

Here $\kappa_o = 0$, $\kappa_{\text{in}} = 1$, and $\kappa_s = 0$, which should be substituted into the results presented in section ‘*General results of model equations*’. Unlike, the step-down scenario considered previously, the step-up case has some interesting steady-state characteristics as discussed in Bolster and Linden (2008). For passive contaminants this steady state corresponds to a uniformly distributed concentration of contaminant equal to that of the source. However, the influence of gravitational settling leads to non-trivial steady-state distributions.

Here we present the transient evolution of average concentration for the step-up case for the same values of α and ζ as we did for the step-down case. The results are plotted in Figure 6. In this case, as we predicted in the discussion on steady states, the evolution of concentrations can be very different. Notice particularly, that for larger particles, $\alpha = 10$, the difference can be quite significant, although the time scales to

reach steady state is comparable. This figure is slightly deceptive in that it makes the low-energy systems appear more efficient at removing large particles, which they are, provided only average concentrations are considered. However, recall that the lower layer concentration is always higher than the well-mixed case, thus exposing occupants to higher levels of contaminant.

Point source

Here we also consider a situation, where a room is initially completely uncontaminated. This time though the contaminant is introduced from a point source. For this case $\kappa_o = 0$, $\kappa_{\text{in}} = 0$, and $\kappa_s = 1$, which can be substituted into the results of section ‘*General results of model equations*’. Once again we track the average concentrations predicted by the three models for various values of settling velocity and interface height. The results are shown in Figure 7.

As with the step-up case we see that both the two-layer models predict similar values. However, these values can differ significantly from those predicted by the well-mixed model (a). For small α as the interface height, ζ , increases the average concentration for the two-layer systems decreases, while the one-layer system remains unchanged, as the average concentration for the two-layer case is $\kappa_{\text{avg}} = \zeta\kappa_l + (1-\zeta)\kappa_u$. Now, from Bolster and Linden (2008) we know that for a point source with small α , the vast majority of the contaminant remains in the upper layer and that the steady state concentration for the upper layer is independent of ζ . Therefore, as the interface height rises, there is less contaminant in the space. As α increases the difference between the upper and lower layer concentrations decreases, because now more particles can fall through to the lower layer. Therefore, the average concentration of the system is closer to that of a well-mixed space. Again, it is worth pointing out that the lower layer concentration is always less than this average and also lower than the well-mixed value.

Numerical method – Germeles algorithm

While the solutions to model (c) above are interesting for comparison purposes, it provides only sufficient information to calculate the average amount of contaminant and provides no description of the contaminant distribution within the upper layer. This model displays stratification of contaminant in the upper layer in a manner that models (a) and (b) do not. The detailed structure of the upper layer is not resolved and, therefore, to determine the vertical concentration profile we can employ a modification of a numerical scheme originally developed by Germeles (1975).

In this scheme, the background ambient fluid is discretized into a finite number of layers, n , and it is

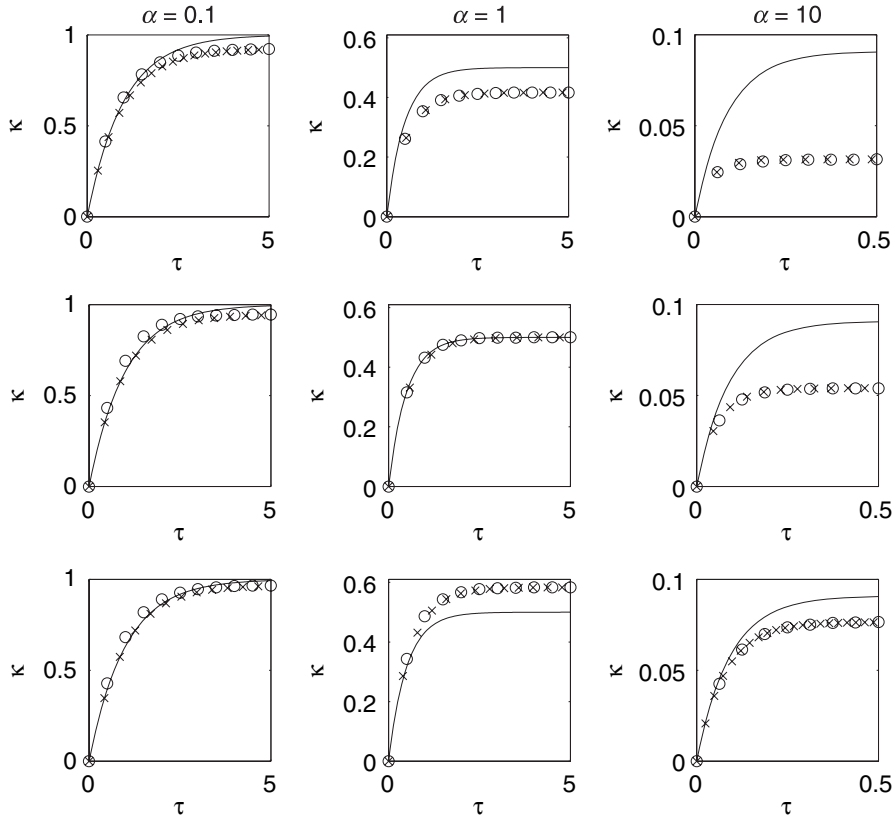


Fig. 6 Step-up case – average concentration for three model with various α and ζ . One-layer well mixed (–), two-layer well mixed (o), two-layer unmixed (x). The top row corresponds to $\zeta = 0.25$, the middle row to $\zeta = 0.5$, and the bottom row to $\zeta = 0.75$

assumed that the plume evolves on a faster timescale than the ambient. Therefore, for any given time step, the equations associated with the plume are solved assuming that the background does not vary. The equations can be solved through the entire height of the room using a Runge–Kutta scheme.

Once the plume equations have been solved the background layers, whose concentration and density remain unchanged during a particular time step, are advected with the background velocity. This process captures the entrainment of fluid from each layer by the rising plume as the advected layers reduce in thickness at each time step. When the plume reaches the ceiling a new layer is added, the thickness of which is determined by the flow rate of the plume at the top of the room and size of the chosen time step. The contaminant concentration assigned to this new layer is the same as the concentration of contaminant in the plume at the top of the room. For details of this numerical method and the plume equations see Bolster and Linden (2007) and Germeles (1975).

Case 1 – step-down

A sample set of solutions for three values of α at various times at an interface of $\zeta = 0.5$ are shown in Figure 8. As expected, when using the Germeles

algorithm, the upper layer is concentration stratified and the well-mixed assumption is questionable. As with passive contaminants (Bolster and Linden, 2007) the interface location plays an important role, always corresponding to the maximum concentration in the upper layer. The biggest difference between this case and passive contaminants is that the concentration at the interface decreases with time. In the passive case there is a front that falls from the ceiling towards the interface, below which the concentration remains that which is initially in the room. For the passive case the descent time of this front to the interface can be shown to be infinite. However, for particulate contaminants, this front will fall more quickly due to gravitational settling and actually reach the interface in finite time. Physically, this can be interpreted as the fact that particles can fall through the interface, whereas passive contaminants cannot. The descent time of this first front, τ_d can be calculated from (18) and decreases with increasing particle size. It approaches infinity as $\alpha \rightarrow 0$.

In addition, the interface always corresponds to the region of maximum concentration, because, if the concentrations in the upper layer fall below those of the lower layer (which does not happen for passive contaminants), the lower layer has the highest concentration levels and thus so does the lower side of

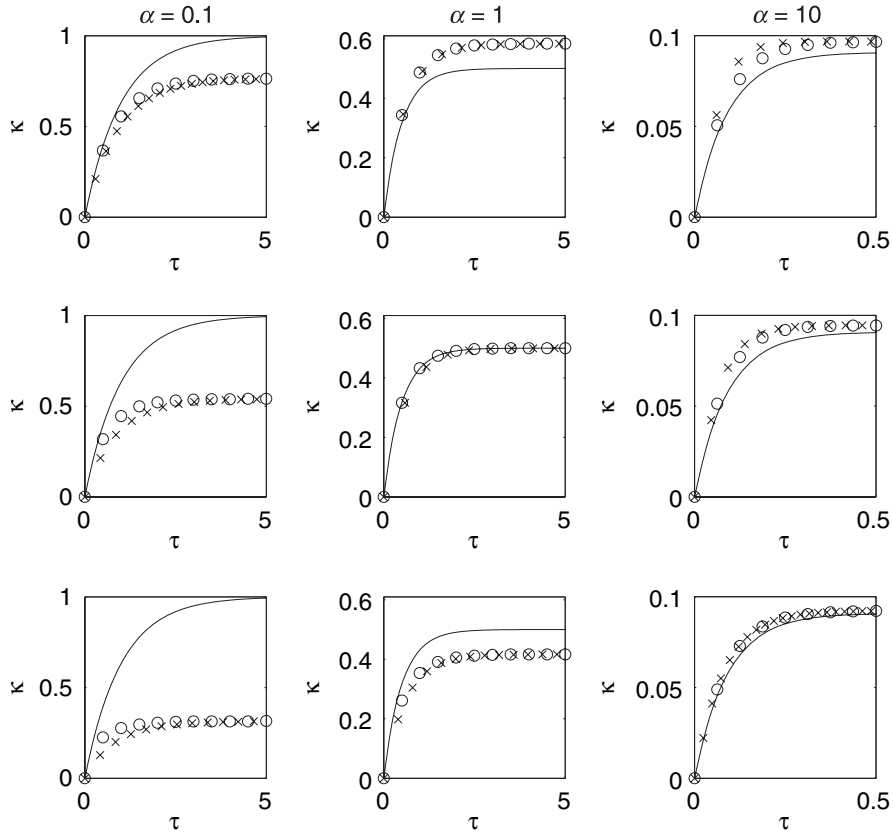


Fig. 7 Point source – average concentration for three model with various α and ζ . One-layer well mixed (—), two-layer well mixed (o), two-layer unmixed (x). The top row corresponds to $\zeta = 0.25$, the middle row to $\zeta = 0.5$, and the bottom row to $\zeta = 0.75$

the interface. From an occupant's perspective this increased exposure in the lower layer and interfacial region is a concern.

Once again, as with passive contaminants, the reason this low-energy ventilation system is not more efficient at contaminant removal than a traditional system can be explained by the plots in Figure 8. Low-energy systems are efficient from a heat removal perspective because the warmest fluid being extracted from the top of the room. However, the location of the warmest fluid does not coincide with the region of maximum contamination. Therefore, this energy-efficient mechanism does not translate across to contaminant removal efficiency.

Case 2 – step-up

A sample set of solutions for the step-up case is shown in Figure 9. Again, notice that during the initial transient stage there can be significant gradients in the concentration field in the upper layer. This time though, the concentration in the upper layer increases with height, because through re-entrainment of contaminant from the background into the plume, the concentration at the top of the room is increasing.

Also note that the upper layer concentration is always less than that of the lower layer, as found at

steady state in Part 1 of this project (Bolster and Linden, 2008). The steady-state values shown in Figure 9 correspond to the previously predicted values. Therefore, if the source of contamination is the inlet of the ventilation system occupants in the lower layer will be exposed to the highest levels of contaminant in the room.

Again, for this case these low-energy ventilation systems do not exploit the same mechanism as they do with heat removal, thus reducing their potential contaminant removal efficiency.

Case 3 – point source

Figure 10 shows the vertical concentration profiles, as calculated with the Germeles algorithm for a point source located in a plume, for various values of α and an interface at half the height of the room. There are significant gradients in the concentration field in the upper layer, particularly at early times. As with the step-up case the concentration in the upper layer increases with height, because via re-entrainment of contaminant from the background into the plume, the concentration at the top of the room is increasing. Therefore, the concentration at the top of the room is the maximum concentration in the upper layer.

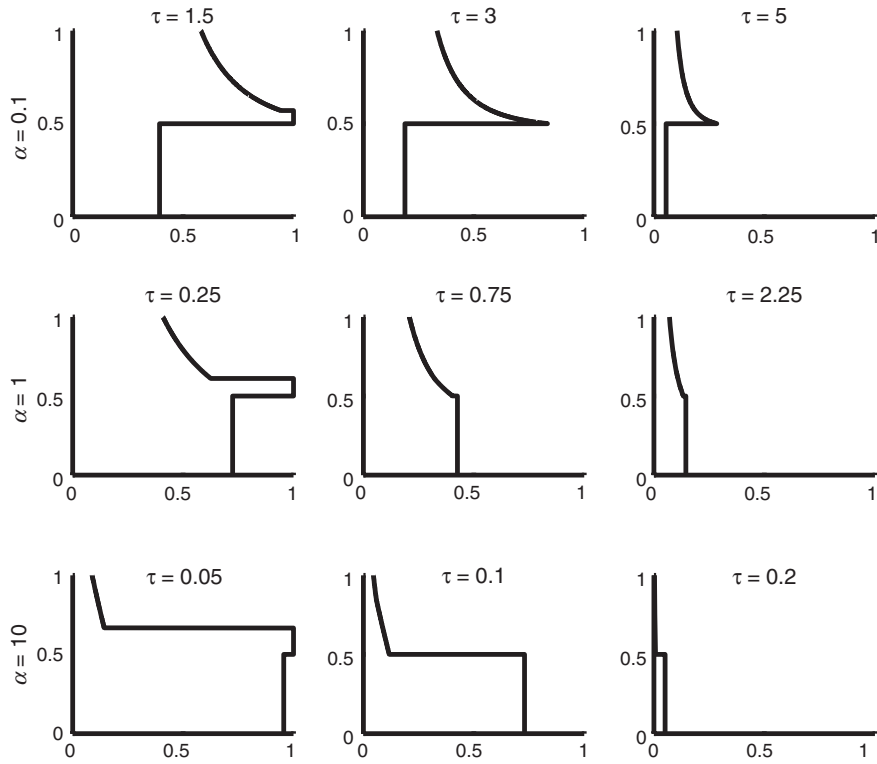


Fig. 8 Step-down Germeles vertical concentrations for $\zeta = 0.5$ over several α at different times

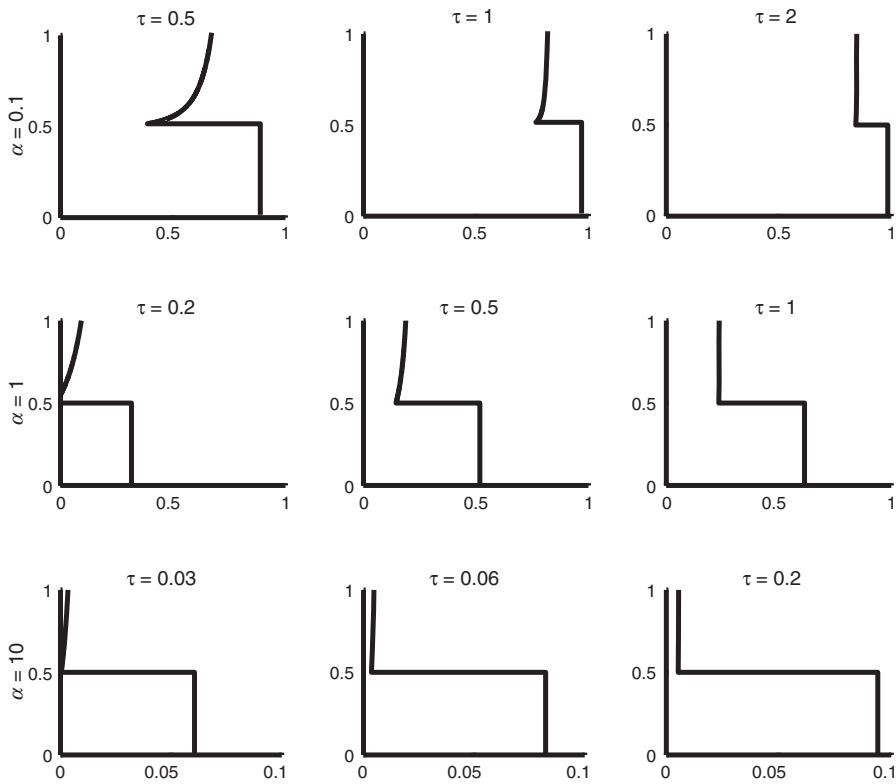


Fig. 9 Step-up Germeles vertical concentrations for $\zeta = 0.5$ over several α at different times

The concentration in the upper layer is also always greater than the concentration in the lower layer. This makes this scenario very different from either of the

previous two. Now, the concentration being extracted from the top of the space is always the maximum concentration in the space. Therefore, the concentration

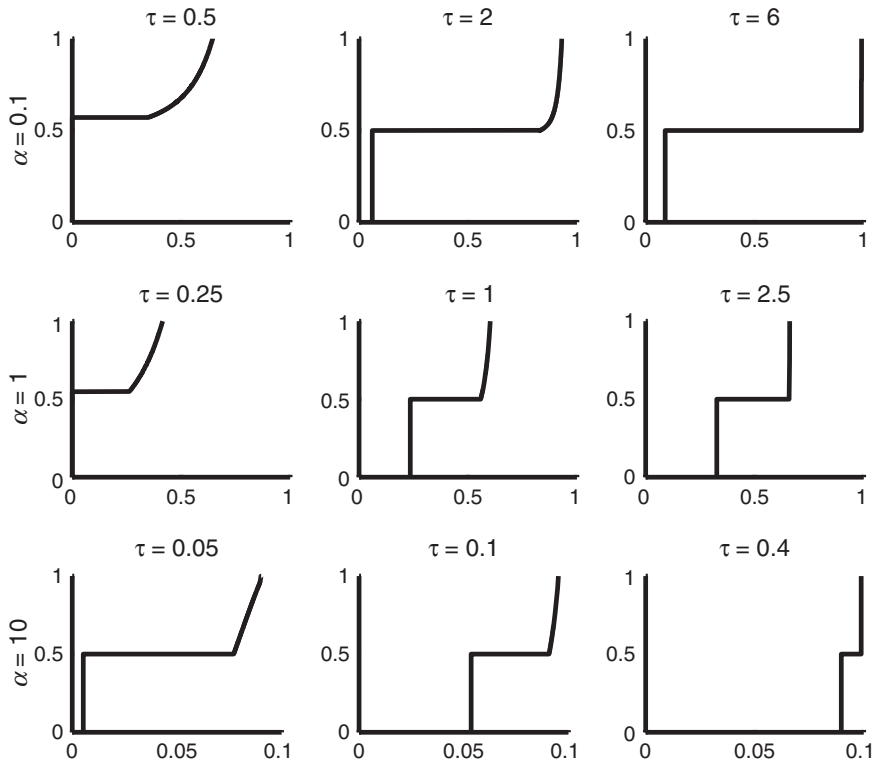


Fig. 10 Point source Germeles vertical concentrations for $\zeta = 0.5$ over several α at different times

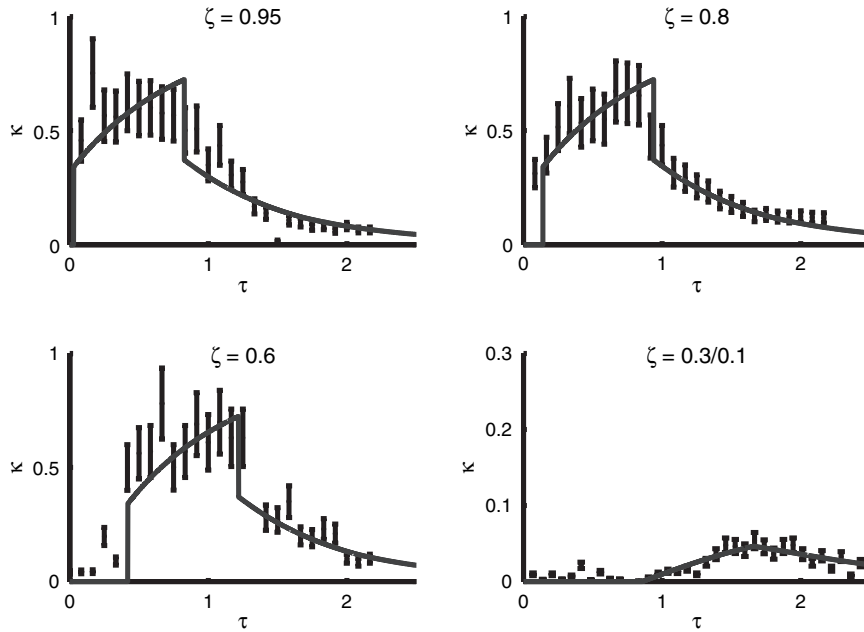


Fig. 11 Experimental results for $\alpha = 0.1$. The solid line represents the theoretically predicted concentration using the Germeles model. The error bars represent the experimental measurements

extraction process is exploiting the same mechanism as the temperature extraction mechanism that makes these low energy systems so appealing. This translates into optimum efficiency of contaminant removal, which can clearly be seen in the previous discussion

on averages and transients in this scenario. Another feature shown in Figure 10 is that ratio of the concentration of upper to lower layers approaches unity as α increases, thus approaching an entirely well-mixed space.

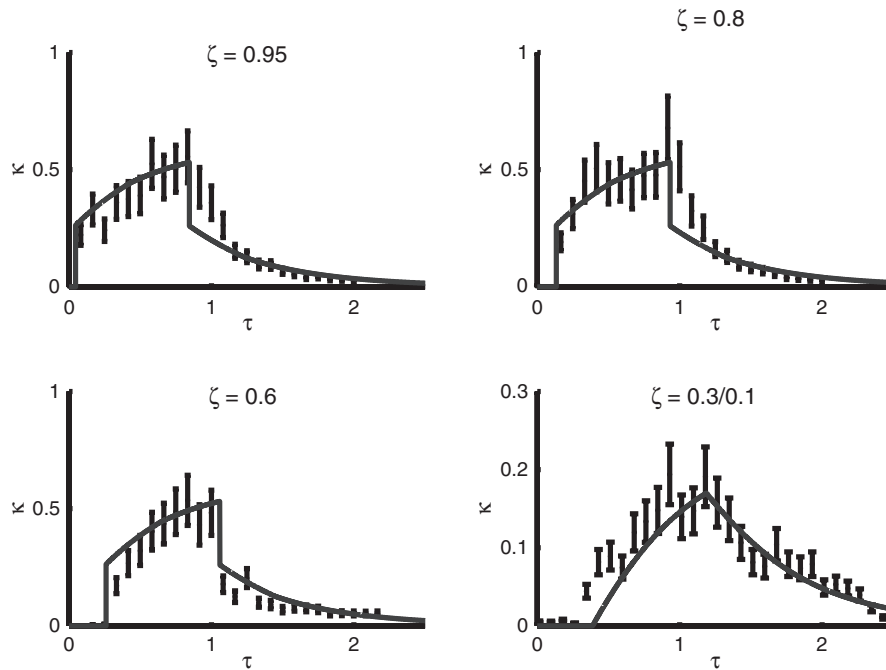


Fig. 12 Experimental results for $\alpha = 0.625$. The solid line represents the theoretically predicted concentration using the Germeles model. The error bars represent the experimental measurements

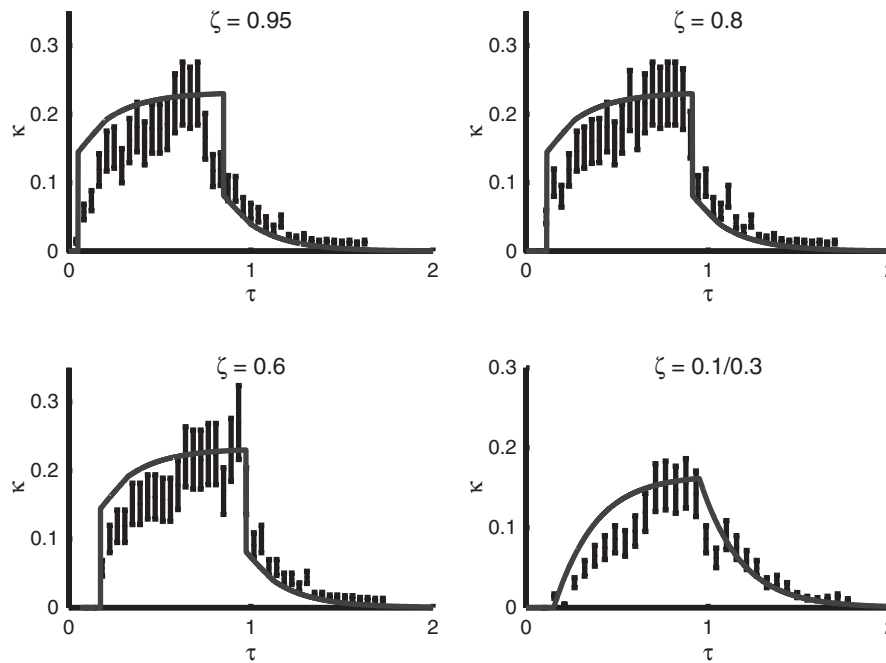


Fig. 13 Experimental results for $\alpha = 2.5$. The solid line represents the theoretically predicted concentration using the Germeles model. The error bars represent the experimental measurements

Experiments

To validate the models presented here and gain further insight into the dynamics of particles in low-energy ventilation systems, a series of full scale laboratory experiments were conducted. A chamber of cross

sectional area 1.3×2.6 m and height 1.8 m was ventilated by a displacement system. Although the experimental chamber is not as tall as a typical interior space, it is large enough to ensure that the main physical processes are represented accurately. A heat source of 65 W is placed in the center of the room. The

temperature in the background was measured at various heights (30, 60, 90, 120, and 150 cm) using type K thermocouples. The heat source consisted of a light bulb, which is encased in a specially constructed wooden enclosure ($0.2 \times 0.2 \times 0.22$ m) to minimize radiative losses. Wrapping the box in materials of low emissivity, such as aluminium foil, had negligible effect on the background temperature and so radiative losses were considered small. Because of the difficulties involved in generating a step-up or step-down situation with particles, the only situation which we consider here is the point source in the plume, which still demonstrates the interesting dynamics associated with this flow.

The interface dividing the upper and lower layers is designed to sit at a height corresponding to half the height of the room (i.e. $\zeta = 0.5$). Three values of $\alpha = 0.1, 0.625,$ and 2.5 are considered. Unfortunately values of $\alpha > 2.5$ were inaccessible with our current equipment. Once the temperature in the room has reached steady state, monodisperse particles of known size are injected vertically in coflow into the plume with a medical nebulizer. The particles used are polystyrene ‘microbead NIST traceable particle size standard’ manufactured by Polysciences Inc. (Warrington, PA, USA) and are manufactured to within a $\pm 2.5\%$ size standard. The flow rate of injection is very small compared with the flow rate in the plume and so its effect is considered to be negligible. Running the nebulizer does not affect the temperature field and so this seems a reasonable conclusion.

The contaminant source was turned on for a certain amount of time $\tau_{\text{on}} = \frac{5}{6}\tau$, where τ is the flushing time (i.e. $\text{Volume}/Q_{\text{in}}$) and then switched off. A model 237A/B Met One Particle Counter (Hach Ultra, Grants Pass, OR, USA) was used to detect and count particles. It is placed at various heights within the room and particle concentrations were measured periodically every 30 s. The particle concentrations are tracked until they return to the background noise levels, so that both the increase and drop in concentrations were captured.

The results of these experiments are shown in Figures 11–13. The error bars on the experimental data are associated with the uncertainty in the measurement of particle concentration and the rate of release by the nebulizer, which corresponds to roughly $\pm 20\%$. In all three cases the qualitative agreement between experiment and models is good. The quantitative agreement is generally within the $\pm 20\%$ error bars. However, there are some regions of larger disagreement and occasional measurements that are quite far off the predicted value. These can stem from external infiltration or some other contaminant source that we could not control in our experiment.

An important feature to note in the experimental data, which is particularly obvious in Figures 11 and 12, is that the upper layer is clearly not well mixed as

there is a measurable time delay in the concentration field at $\zeta = 0.6$ compared to $\zeta = 0.95$ associated with the advection of particles from the top of the room to that height. Experimentally, this time delay is not so obvious for the larger particles (i.e. $\alpha = 2.5$) because, as a result of faster settling, the time for particles to descend becomes comparable to the measurement time and so the concentration fields for the three upper values of ζ become indistinguishable.

In addition, for the largest particles, there seems to be a delay in the experimental data for the initial rise of concentration in the upper layer compared to the theoretical prediction. The peak-predicted value is comparable, but the time taken to get there is longer. This is probably, because we neglect the effect of settling within the plume. The present models predict an instant increase in concentration once the source is turned on. This comes from the assumption that the plume time scale is much faster than that of the background, which is true. However, there may be a lag in this because of settling effects. This theoretical over-prediction of the upper layer concentration also leads to an over-prediction of the lower layer concentration.

Conclusion

In this paper, we have considered the transient transport of particulate contaminants in a displacement-ventilated space. We compared three models, one representing a traditional ventilation system and the other two representing the displacement-ventilated space. We considered three types of contamination scenarios, namely a step-down, a step-up and a point source contaminant. Several important differences between the traditional and low-energy systems were noted.

While for passive contaminants it is often argued that studying one of the step-up, step-down and point source contamination scenarios is equivalent to studying them all, this is not the case for particulate contaminants and the low-energy displacement system described here. The influence of gravitational settling is to introduce an ‘irreversibility’ or ‘preferential direction’ to the flow, which destroys the symmetry of the step-up, step-down and point source methods. Therefore, it is important to understand the differences between these three scenarios as each one gives important information about real contamination scenarios. The governing equations presented in this paper are all linear and, therefore, each scenario can be studied separately, and superposition of solutions can be used to study more complex situations.

It is widely believed that low-energy displacement ventilation systems can be better than traditional mixing systems at removing contaminants from a space. This is because there is a belief that these systems will use the same mechanism for contaminant

removal as they do for heat removal, where they are clearly more efficient. The heat extraction problem exploits the natural stratification that develops, extracting the warmest air that naturally sits at the top of the room. However, there is no physical justification as to why this location should correspond to the location of maximum contaminant concentration too. In fact many times it does not (Bolster and Linden, 2007).

For the step-down case we considered the quantity of particles deposited to the floor as an indicator of the fraction of contaminant that an occupant has been exposed to. For smaller particles and low interfaces (i.e. small α and ζ) the low-energy displacement system performs better than the traditional mixing system. However, for larger particles this index indicates that the low-energy systems cause higher levels of exposure. Allowing for gradients in the upper layer [i.e. model (c)] leads to higher exposure than the well-mixed upper layer, because the concentration at the interface is higher than at the top of the room (like the passive contaminant case in Bolster and Linden, 2007), thus allowing higher concentrations to settle back down to the lower layer.

Similarly for the step-up case, we showed that, at steady state, the concentration in the lower layer is greater than that of the upper layer. This is because the level of maximum concentration is in the lower layer, but the level of air extraction is in the upper layer, thus not exploiting the ‘energy’ benefit displacement ventilation offers where the warmest air is extracted at the top of the room.

On the other hand, when considering the point source scenario, we predict a higher steady-state concentration in the upper layer compared with the lower layer. The lower layer concentration will always be less than that in an equivalent traditional system,

thus reducing occupants’ exposure to contaminants. Here, unlike the step-up and step-down cases, the situation exploits the same mechanism as the heat removal problem, always extracting the most contaminated air from the top of the room.

As mentioned in Part 1 of this work, the information obtained in this work clearly has an impact on the design of an effective ventilation system and the specific design requirements. In some cases a displacement system may provide better air quality than a traditional mixing ventilation system. On the other hand, if we consider a naturally ventilated space, where external sources can play an important part in contamination, the step-up scenario may be relevant and a mixing system could be preferred.

Finally, one point that should hopefully be clear from both Part 1 and Part 2 of this work is that it is not sufficient to know the average concentration of contaminant in a space, both from an exposure and from a modeling perspective as such limited knowledge can lead to over- and under-predictions of contaminant concentrations, which in turn can lead to over- and under-designed ventilation systems, which can be wasteful of energy or not adequate in terms of indoor air quality. Integrating models such as those presented here can aid in better design. In addition, there is no reason to believe that the models presented here could not be developed to include further transport mechanisms associated with important contaminants (e.g. chemical reactions, VOC transport, etc.).

Acknowledgement

The authors would like to thank the California Energy Commission for their financial support of this project.

References

Bolster, D. and Caulfield, C. (2008) Transients in natural ventilation – a time periodically varying source, *Build. Serv. Eng. Res.*, **29**, 119–135.

Bolster, D. and Linden, P. (2007) Contaminants in ventilated filling boxes, *J. Fluid Mech.*, **591**, 97–116.

Bolster, D. and Linden, P. (2008) Particle transport in low energy ventilation systems. Part 1: Theory of steady states, *Indoor Air* (submitted).

Cook, M., Ji, Y. and Hunt, G. (2003) Cfd modelling of natural ventilation: combined wind and buoyancy forces, *Int. J. Ventilation*, **1**, 169–180.

Feustel, H. (1999) Comisan international multizone air-flow and contaminant transport model, *Energy Build.*, **30**, 3–18.

Germeles, A.E. (1975) Forced plumes and mixing of liquids in tanks, *J. Fluid Mech.*, **71**, 601–623.

Holmberg, S. and Li, Y. (1998) Modelling of the indoor environment particle dispersion and deposition, *Indoor Air*, **8**, 113–122.

Hunt, G. and Kaye, N. (2006) Pollutant flushing with natural displacement ventilation, *Build. Environ.*, **41**, 1190–1197.

Ji, Y., Cook, M. and Hanbya, V. (2007) Cfd modelling of natural displacement ventilation in an enclosure connected to an atrium, *Build. Environ.*, **42**, 1158–1172.

Lambert, W., Samet, J. and Spengler, J. (1993) Environmental tobacco smoke concentrations in no-smoking and smoking sections of restaurants, *Am. J. Public Health*, **83**, 1339–1341.

Linden, P.F., Lane-Serff, G.F. and Smeed, D.A. (1990) Emptying filling boxes: the fluid mechanics of natural ventilation, *J. Fluid Mech.*, **212**, 309–335.

Musser, A. and Persily, A. (2002) Multizone modeling approaches to contaminant based design, *ASHRAE Trans.*, **108**, 1–8.

Ozkaynak, H., Ryan, P., Allen, G. and Turner, W. (1982) Indoor air quality modeling: compartmental approach with reactive chemistry, *Environ. Int.*, **8**, 461–471.

Rodes, C., Kames, R. and Wiener, R. (1991) The significance and characteristics of the personal activity cloud on exposure assesment measurements for indoor contaminants, *Indoor Air*, **2**, 875–891.

- Schneider, T., Kildeso, J. and Breum, N. (1999) A two compartment model for determining the contribution of sources, surface deposition and resuspension to air and surface dust concentration level in occupied spaces, *Build. Environ.*, **34**, 583–595.
- Yan, Z. (2007) Large eddy simulations of a turbulent thermal plume, *Heat and Mass Transfer*, **43**, 503–514.
- Zhang, Z. and Chen, Q. (2006) Experimental measurements and numerical simulations of particle transport and distribution in ventilated rooms, *Atmos. Environ.*, **40**, 3396–3408.
- Zhao, B., Li, X. and Zhang, Z. (2004) Numerical study of particle deposition in two differently ventilated rooms, *Indoor Built Environ.*, **13**, 443–451.

Appendix A. Concentration at top of room

When a new layer forms at the top of the room it has $[Q_p(z = H)]\Delta t$ fluid being supplied to it by the plume and $(Q_{out})\Delta t$ being extracted by the vent. The size of the new layer, because of gravitational settling, is $[Q_p(z = H) + Q_f - Q_{out}]\Delta t$. Therefore, assuming perfect mixing in this new layer the concentration of this new layer will be

$$C = \frac{Q_p}{Q_p + Q_f} P(z = H), \quad (\text{A.1})$$

which can readily be shown to be

$$C = \frac{1}{1 + \frac{3\alpha\zeta}{5-2\zeta}} P(z = H). \quad (\text{A.2})$$